



Finite element modeling of plain weave fabrics from photomicrograph measurements

E.J. Barbero^{a,*}, J. Trovillion^b, J.A. Mayugo^c, K.K. Sikil^d

^a Mechanical and Aerospace Engineering, West Virginia University, 325 ESB, Morgantown, WV 26505-6106, United States

^b Construction Engineering Research Laboratory, Champaign, IL, United States

^c University of Girona, Spain

^d West Virginia University, 325 ESB, Morgantown, WV 26505-6106, United States

Available online 21 March 2005

Abstract

The aim of this work is to develop accurate finite element models of plain weave fabrics to determine their mechanical properties. This work also aims at developing a method for describing the internal geometry from actual measurements of tow geometry made on photomicrographs of sectioned laminates. The geometric models needed for finite element discretization of the plain weave fabrics are developed for a variety of plain-weave reinforced laminates for which experimental data is available in the literature. These include single lamina composites from three sources, as well as laminates in iso-phase and out-of-phase configurations. The procedures to determine all the elastic moduli using iso-strain, iso-stress, and classical lamination theory are presented. Comparisons with experimental data and with predictions using the periodic microstructure model are provided in order to support the validity of the proposed models.

© 2005 Elsevier Ltd. All rights reserved.

Keywords: Composite; Fabric; Modeling; Experimental; Plain weave; Optical; Geometry; Microstructure

1. Introduction

Unidirectional laminated composites exhibit excellent inplane properties but poor inter-laminar properties because there are no reinforcements in the thickness direction. This leads to poor damage tolerance and poor impact resistance when inter-laminar stresses are present. To overcome these problems, plain weave fabrics are used as reinforcements in composites in order to obtain balanced ply properties and improved inter-laminar properties. These advantages are realized at the cost of reduced stiffness and strength in the inplane directions. Therefore, it is important to study the mechanical behavior of such composites in order to fully realize their potential.

A fabric is a collection of fiber tows arranged in a given pattern. Both fibers and matrix are responsible for bearing the mechanical loads while the matrix protects the fibers from environmental attack [1]. Fabrics are classified as woven, non-woven, knitted, or braided [2]. Further, they can also be classified into 2-D (two-dimensional reinforcement) and 3-D fabrics (three-dimensional reinforcement). Some examples of fabrics are plain weave, satin weave, weft knitted, warp knitted, and orthogonal fabrics.

The stiffness and strength of fabric-reinforced composites are controlled by the fabric architecture and material properties of fiber and matrix. The fabric architecture depends upon the undulation, crimp, and density of the fiber tows. A tow is an untwisted strand of fibers. The undulation or waviness of the tows causes crimps (bending) in the tows, which significantly reduces the mechanical properties of the composite. The geometry of the

* Corresponding author. Tel.: +304 293 3111; fax: +304 293 6689.
 E-mail address: ever_barbero@mail.wvu.edu (E.J. Barbero).

woven composite is complex and the choice of possible architectures is unlimited. The present work concentrates on modeling the elastic behavior of plain weave fabrics, using optical microscopy and the finite element method.

Plain weave fabrics are formed by interlacing or weaving two sets of orthogonal tows. The tows in the longitudinal direction are known as warp tows. The tows in the transverse direction are known as the fill tows or weft. The interlacing causes bending in the tows, called tow crimp.

Plain weave fabrics can be arranged in different laminate stacking configurations. A single lamina consists of warp and fill tows surrounded by matrix in a single layer as shown in Figs. 1 and 2. The iso-phase configuration consists of plain weave laminae arranged one above the other so that the undulations are in phase. The out-of-phase configuration consists of plain weave laminates arranged in a symmetric manner, so that the

undulations are out of phase by a , which is the pitch of the undulation (Fig. 1). In order to model the single lamina, iso-phase, and out-of-phase laminates using finite element methods, only the representative volume elements (RVE) of the respective configurations are considered. The RVE is the repeating element (unit cell) that represents the whole composite fabric structure (Fig. 1).

Numerous methods are available for modeling and analyzing plain weave fabric composites. There are two main categories: analytical models and numerical models. Chou and Ito [9] developed 1-D analytical models of the plain weave laminated composites for determining their mechanical properties. The undulation of the fill tow was not considered for the analysis. Three different laminate stacking configurations were considered for the analysis: iso-phase, out-of-phase and random phase laminates. Mathematical models of the configurations were explained very well and predictions of inplane modulus are compared to experiments for all three configurations. The undulation of warp tow was assumed to be sinusoidal and two types of cross-section were assumed for the fill tows: sinusoidal and elliptical. The iso-strain condition was used for evaluating the stiffness of the plain weave laminates.

Ishikawa and Chou [10,11] developed three models to predict the elastic properties of woven fabric laminates. The mosaic model [10] was used to predict the stiffness of satin weave fabric composites. The model neglects the tow crimp and idealizes the composite as an assemblage of asymmetric cross-ply laminates. Then, an iso-stress or iso-strain condition was used to predict the stiffness of the laminate depending on whether the laminates are assembled in series or parallel. Since the model neglects the tow crimp, the prediction of stiffness is not

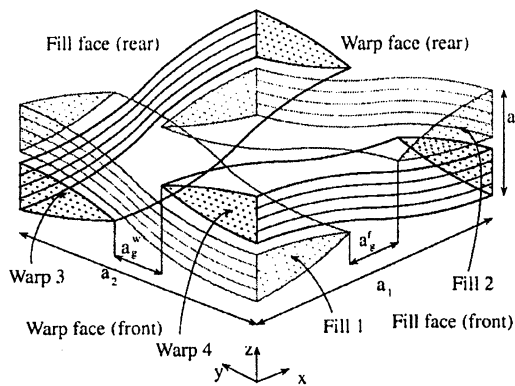


Fig. 1. Schematic representation of the Fabric geometry.

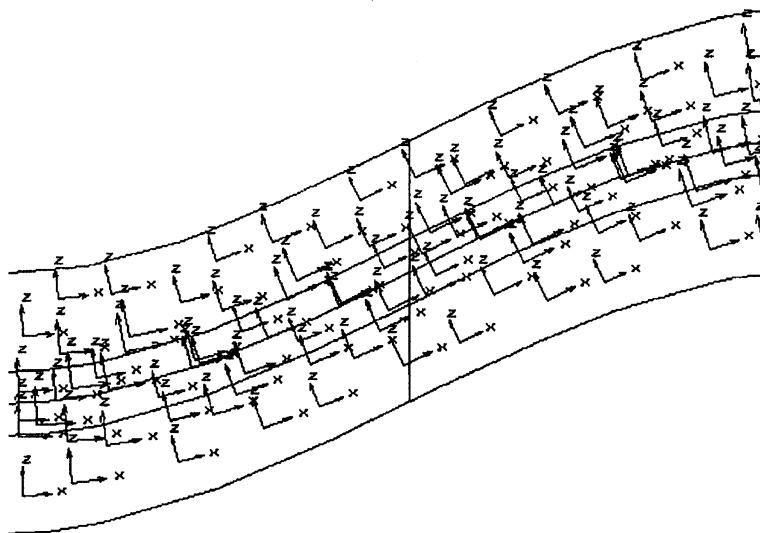


Fig. 2. Material orientation inside a tow.

accurate. The fiber undulation model [10] or the 1-D model considers fiber undulation in the longitudinal direction but neglects it in the transverse direction. The bridging model [11], a combination of mosaic and fiber undulation model, was developed for satin weave fabrics. The model reduces to the crimp model [10] for plain weave fabrics and hence the stiffness prediction is not accurate.

Most analytical models are based on classical lamination theory (CLT). Huang [3] developed a micromechanics bridging-model to predict the elastic properties of woven fabric composites. The geometric models of the fabrics (RVE) were well described. The tow cross-section was assumed to be elliptical and a tow undulation was described by a sinusoidal function. A discretization procedure was applied to the RVE of the fabric composite. The RVE was divided into a number of sub-elements, with no divisions in the thickness direction as shown in [3]. Each sub-element consists of the tow segments and the pure matrix. The tow segments were considered as unidirectional composites in their material co-ordinate system. The elastic response (compliance) of the tow segments and the matrix were assembled in order to get the effective stiffness of the sub-element using classical laminate theory (iso-strain condition). The overall elastic property of the RVE was calculated by assembling the compliance matrix of the sub-elements under iso-stress assumption.

Naik and Ganesh [4] developed 2-D micromechanical models of plain weave fabrics to determine the elastic properties of the fabrics, taking the warp and weft tow undulation into consideration. In the case of the slice array model (SAM), the RVE was divided into number of slices. These slices were idealized in the form of four-layered laminate (asymmetrical cross ply sandwiched between matrix layers at top and bottom). The properties of each slice were calculated from the individual layers (considering the undulation), which in turn were used for calculating the elastic constants of the RVE. The limitation of the model is that it approximates the stiffness contribution from the warp strand. This is because the undulation angle for the warp strand is approximated. In order to overcome these limitations, Naik et al. developed the element array model (EAM), including the series-parallel (SP) and the parallel series (PS) models. In the SP model, the slicing was made in the warp direction. Each slice was further divided into elements of infinitesimal thickness. Then, the elastic constants of the warp and fill tows were calculated within each element (considering the undulation angle), and then the stiffness of the element was calculated using the classical laminate theory. The compliance of the slices was calculated from the element stiffness matrix using iso-stress conditions. Finally, the overall stiffness of the RVE was calculated from stiffness of the slices using iso-strain condition. In the PS model, the slicing was made in the fill direction. So, the elements in the slices were assembled using the

iso-strain condition to get the slice stiffness and then the slices were assembled assuming iso-stress condition in order to obtain the overall stiffness of the RVE. Although these models showed good correlation with the experimental data, they are very complicated.

Vandeurzen et al. [5,6] developed analytical, elastic models for 2-D “hybrid” woven fabrics. Three groups of geometric parameters were identified for describing the 2-D weave geometry. The first group is the “know” group, which contains the data supplied by the weaving company- number and diameter of fibers, and tow spacing. The second group is called the “measure group”, which contains quantities that can be obtained from microscopic observations and calculations- aspect ratio of the tows, thickness of the fabric laminate, tow-packing factor, and so on. The third group is called the “calculate group”, which contains the parameters that can be calculated from the know- and measure-group, i.e., fiber volume fraction, orientation of the tows, and so on. The geometric analysis was implemented in a custom application software for Microsoft Excel called TEXCOMP, which was not available for the present investigation. The models work well for prediction of elastic modulus but the prediction of inplane shear modulus is not good.

Hahn and Pandey [7] developed an analytical model to predict the elastic properties of plain weave fabrics. The mathematical functions describing the tow profiles and geometry were provided in detail. The cross-sectional and the undulation were assumed to be sinusoidal. Further, the undulation shape of a tow determines the cross-section shape of a perpendicular tow. The volume fraction of voids was taken into consideration while calculating the volume fraction of fibers, which was neglected by previous investigators. The iso-strain condition was used for calculating the stiffness matrix of the woven fabric. First, the tow stiffness components in material coordinate system were calculated using micromechanics equations. Then the overall stiffness was obtained by averaging the stiffness matrix of tow and matrix over their thickness.

Scida et al. [8] developed an analytical model called MESOTEX (MEchanical Simulation Of TEXtiles) based on classical lamination theory (CLT) to predict the 3-D elastic properties, continuum damage evolution, and strength of woven fabric composites. The properties were calculated by discretization process of the tows and matrix in the unit cell as done by the previous investigators. The calculated stiffness was compared with experimental data and other models. The software was not available for the present investigation.

While the closed form solutions described so far provide simplified stress-strain distributions, numerical models provide detailed stress-strain distributions. The geometrical description of the unit cell architecture with the tows and matrix is the most important aspect in finite element analysis of fabric-reinforced composites.

Mathematical models have been developed to describe the geometry of a unit cell. Averill et al. [12] developed a simplified analytical/numerical model for predicting the elastic properties of plain weave fabrics. The unit cell of the fabric was discretized with brick elements, with one element through the thickness of the cell. The tow volume fraction and tow inclination were calculated based on the assumed unit cell geometry. The stiffness properties of each element were calculated from the fiber volume fraction, orientation of fibers, and fiber and matrix properties using effective moduli theory. These properties were given as input to the finite element model and the overall properties of the unit cell were obtained by applying necessary boundary conditions. The model is simple in the sense that 3-D modeling of tows is not required. Therefore, a fewer number of elements are required for the model and hence the computational time is small. The model yields good results for the stiffness values except for inter-laminar shear modulus G_{13} .

Blackletter et al. [13] developed a 3-D finite element model of a plain weave fabric. The tows and matrix were modeled using PATRAN. Hexahedral elements were used for generating the mesh. The tows were modeled as unidirectional composite materials. The tow properties were calculated using two-dimensional generalized plane strain micromechanics analysis. The model is based on our assumed, idealized geometry that might not describe the actual geometry accurately.

Collegal and Sridharan [14,15] developed two types of finite element models for plain weave fabrics. The first type is similar to the previous finite element models where the quarter model of the RVE, containing the tows and matrix, is meshed using 3-D solid elements. The second type is different from the usual models. Here the model consists of plate elements representing the tows and 3-D solid elements representing the matrix sandwiched between the tows. Thus, the unit cell consists of four plate elements representing fill and warp tows. The thickness variations in the tows were incorporated in the plate elements. Elastic responses of the two models match well with experimental data.

Although a number of models are available for predicting mechanical properties of plain weave fabric rein-

forced composites, each model has its limitations. For example, all CLT-based models under-predict the shear moduli because of the rule of mixtures assumption intrinsic to CLT. Therefore, the aim of this work is to develop accurate finite element models of plain weave fabrics to determine their mechanical properties without these limitations. An accurate model must represent the geometry of the tow with fidelity to the actual composite. Therefore, this work also aims at developing a method for describing the geometry from actual measurements of tow geometry. Comparisons are presented of predicted properties of the fabric-reinforced lamina and laminate vs. experimental data, as well as vs. analytical and approximate results.

2. Two-dimensional geometric models

The geometrical model for the representative volume element (RVE, Fig. 1) of plain weave fabrics was developed using the geometrical parameters measured by CERN [16]. The RVE consists of four intertwined tows surrounded by the matrix (isotropic). There are four volumes depicting the tows in Fig. 1. Two of them represent two half tows in the x -direction (warp tows) and the remaining two represent two half tows in the y -direction (fill tows). Each volume (tow) is modeled as a unidirectional composite with orthotropic properties in the material coordinate system that follows the tow undulation (Fig. 2).

The 2-D geometric model describing the internal geometry of the RVE of a single lamina is developed from measurements taken on photomicrographs of the faces of the RVE. Photomicrographs of the fill and warp faces are shown in Figs. 3 and 4, respectively [16,17]. The parameters describing the geometry are shown in Fig. 5. From photomicrographs of the RVE faces (Figs. 3 and 4), the bounds of the tows in the fill cross-section (Fig. 3) and warp cross-section (Fig. 4) were digitized using GRABIT, a macro in Excel that allows us to record coordinates of selected points from a digital picture. A series of coordinate data points were recorded along the boundaries of the three tows seen in each

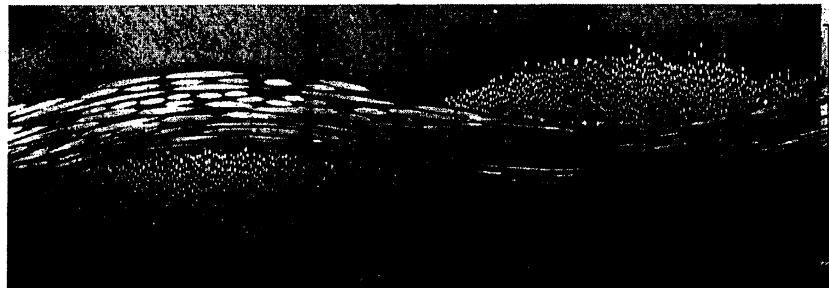


Fig. 3. Photomicrograph of the (rear) fill face of the fabric of CERN.

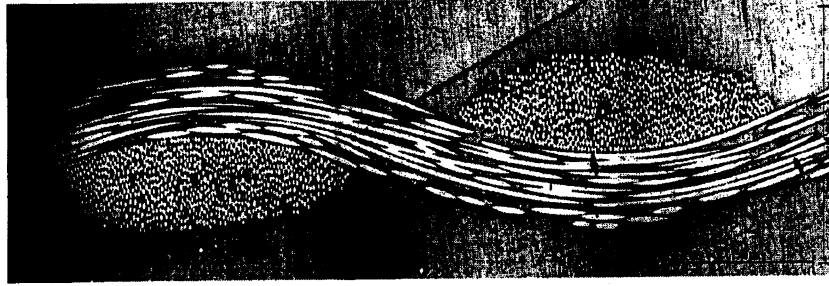


Fig. 4. Photomicrograph of the (rear) face of the fabric of CERL.

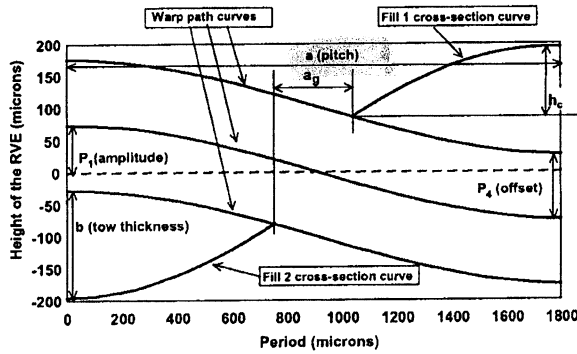


Fig. 5. Schematic representation of one face of the representative volume element from measured tow parameters.

image (Figs. 3 and 4). The data points were then fitted to a sinusoidal function as follows:

$$y = P_1 \sin(P_2 x + P_3) + P_4 \quad (1)$$

where P_1 is the amplitude of the tow path curve in millimeters, $P_2 = \pi/a$, a is the pitch of the tow path curve in millimeters, P_3 is the phase adjustment factor, $P_4 = b/2$ is the offset depicted in Fig. 5 in mm, b is the tow thickness in mm, and

$$h = 2(P_4^w + P_4^f) \quad (2)$$

is the thickness of the RVE in mm (equal to a_3 in Fig. 1), where the superscripts 'f', 'w', indicate fill and warp, respectively. The phase adjustment factor P_3 is used to adjust Eq. (1) to the tow boundary when the peak of the tow shown in the photomicrograph does not coincide with the origin of the RVE. These values are mea-

sured in the warp and fill directions since the shape and size of the tows are different in these two directions.

Four sinusoidal curves of the form of Eq. (1) are generated from each photomicrograph. The equations are plotted to verify that the curves from the warp and fill directions match (do not overlap nor gap exists). Using data from actual photomicrographs, the curves in the warp direction did not match with the curves in the fill direction due to slight discrepancies among the photomicrograph measurements on the faces of the RVE. Hence, the amplitude of the curve P_1 was adjusted in the fill direction so that the curves in the two directions match [17]. The measured parameters for developing the 2D geometrical model of the RVE are shown in Table 1.

Similarly, 2-D geometric models of the RVE for single lamina, iso-phase, and out-of-phase laminates are developed from the tow parameters measured in [9] (Table 2), which are different from those measured by CERL [16].

Table 2
Geometric parameters for iso-phase and out-of-phase laminates [9] (Fig. 5)

Geometrical parameter	Single-lamina and iso-phase laminate [mm]	Out-of-phase laminate [mm]
Pitch, warp direction (a^w)	3.216	3.204
Gap width, warp direction (a_g^w)	0.392	0.391
Pitch, fill direction (a^f)	3.055	3.095
Gap width, fill direction (a_g^f)	0.275	0.366
Tow thickness (b)	0.318	0.315
Lamina thickness (h')	0.636	0.630

Table 1
Parameters describing a single lamina as measured by CERL [16] from photomicrographs

Direction of measurement	Type of curve	Domain where valid	P_1 (mm)	P_2 (mm ⁻¹)	P_3 (rad)	P_4 (mm)
Warp direction XY plane, $y = f(x)$	Warp path	$0 < x < 1.836$	0.07442	1.710	1.5707	0.10130
	Fill 1 cross-section	$0 < x < 0.770$	0.26361	1.296	1.5707	0.05807
	Fill 2 cross-section	$1.11 < x < 1.836$	0.26361	1.296	-0.8138	-0.05807
Fill direction YZ plane, $z = f(y)$	Fill path	$0 < y < 1.836$	0.11657	1.726	1.5707	0.08967
	Warp 1 cross-section	$0 < y < 0.630$	0.24177	1.680	1.5707	0.06604
	Warp 2 cross-section	$1.19 < y < 1.836$	0.24177	1.680	-1.5535	-0.06604

3. Three-dimensional geometric modeling

The 3-D geometric models are created using I-DEAS™, Version.8, which is simple to use, has an interactive graphic user interface (GUI) with menus that are easy to work with, and offers features like creating volume from set of curves, partitioning of solids, material orientation features, and so on.

The procedure for developing 3-D geometric models of a single lamina is based on the 2-D geometric model. First, the path curves and the cross-section curves (Fig. 5) describing the tows in the warp and fill direction are drafted from the measured parameters (Tables 1 and 2) and Eq. (1) of the 2-D geometric model using the function spline option in I-DEAS™. Sweeping operations of cross-section curves along path curves could not be performed because, starting at the front faces and sweeping towards the back faces following the warp and fill path curves, the fill (and warp) cross-section curves did not match the fill (and warp) cross-section curves in the back faces of the RVE. This is due to the fact that the fill (and warp) cross-section curves on the back face are not identical to those on the front surface because they have to conform to the shape of the warp (and fill) tows. Therefore, the cross-section curves from

the front face are mirrored (rotated by 180°) and copied onto the back faces of the RVE (Fig. 6). Then, the surfaces are created in IDEAS™ by blending the cross-section and path curves that define the tow surfaces in the warp and fill directions. Three path curves and four cross-section curves are required in order to define the surfaces of each tow, as shown in Fig. 6. Surfaces related to the warp (and fill) are stitched together to get a solid model of the tows. In total, four intertwined volumes are obtained with two of them in the warp direction and two in the fill direction. The solids generated in IDEAS™ to represent the tows may intersect when the surfaces are stitched together. This is due to the interpolation of analytical functions (Eq. (1)) using splines, which is performed by I-DEAS™ when the surfaces are formed. To avoid tow intersections, which do not occur in the real composite, a slight rotation of the fill tows about the warp axis is introduced. This procedure may create a very small gap between tows, which is modeled as matrix (0.00524 mm gap when modeling the fabric of [8]). The volumes are then partitioned from a rectangular prism having the dimensions of the RVE, which indicates to the software that there are four volumes inside the prism. This is visualized as four half tows surrounded by matrix, as shown in Fig. 7.

The iso-phase and out-of-phase laminate configurations [9] are modeled by making eight copies of the single lamina, then stacking and joining them into an eight-layer laminate, using the move and join operations in I-DEAS™. For the out-of-phase laminate [9], the geometric model consists of eight plies, with the laminae arranged in a symmetric manner.

4. Finite element modeling

The 3D geometric models are meshed using 10 node solid parabolic tetrahedral elements under the free mesh option in I-DEAS™. Each node has 3 degrees of freedom, u_x , u_y , and u_z . The elements exhibit a quadratic

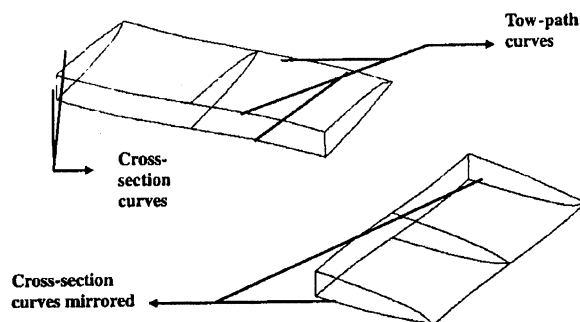


Fig. 6. Description of tow-path and cross-section curves used to generate the tow surfaces with I-Deas™ software.

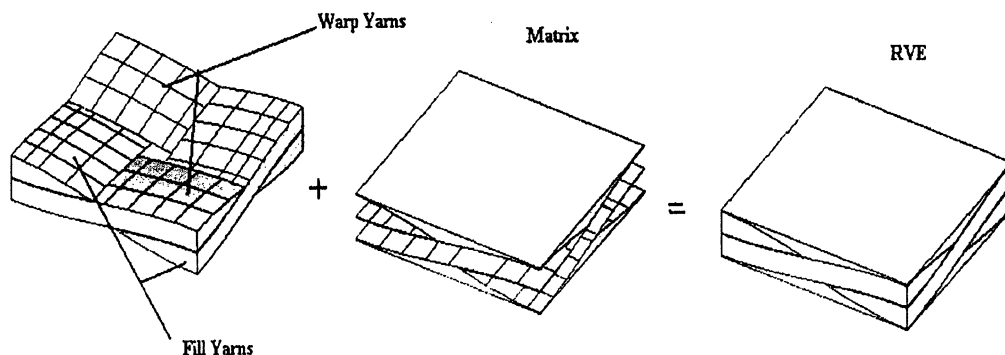


Fig. 7. 3-D views of a plain weave fabric.

displacement behavior, which is well suited for modeling the complex and irregular structure of the plain weave fabric. The mesh is checked for distortion. A mesh sensitivity analysis is performed in order to get accurate results.

The material properties of the tows vary along the orientation of the path curve. Therefore, the material orientations of tow elements are made to follow the path curve using the material orientation option. The local x -direction of the coordinate system for each element follows the path curves of the warp or fill tows (depending on the tows for which material orientation is being defined) using the material orientation option in I-DEASTM (Fig. 2). The x -direction of the tow elements indicates the fiber direction, the y -direction indicates the transverse inplane direction of the RVE, and the z -direction indicates the thickness direction as shown in Fig. 2.

The FE models of the plain weave fabric are exported to ANSYSTM through a text file. While exporting, the element type is changed to Solid 92, which is a quadratic element in ANSYSTM. There were several errors encountered while opening the file in ANSYSTM. The ANSYSTM software supports two types of Poisson's ratio, major Poisson's ratio and minor Poisson's ratio, for orthotropic material model. The major Poisson's ratio (PRXY, PRYZ, PRXZ) corresponds to ν_{xy} , ν_{yz} , ν_{xz} as input. The minor Poisson's ratio (NUXY, NUYZ, NUXZ) corresponds to ν_{yx} , ν_{zy} , ν_{zx} as input. When the file is exported from I-DEASTM, ANSYSTM interpreted ν_{xy} , ν_{yz} , ν_{xz} as minor Poisson's ratio instead of major Poisson's ratio. This resulted in error when the software verified for the restrictions on elastic constants. Substituting PR for NU corrects this in the ANSYSTM command lines. Once the errors are corrected, the model is solved.

Transversely isotropic material properties are assigned to the tow elements and isotropic properties are assigned to the matrix elements. The material properties of the tows are calculated using micromechanics [18,19] depending on whether the fibers are isotropic or transversely isotropic. The volume fraction and elastic properties of fiber and matrix for all the materials are given in Table 3. In addition, a volume correction had to be done for the modeling the fabric in [9], as explained next.

The fiber volume fraction in the tow V_f is necessary to calculate the tow properties using micromechanics.

Although the tow volume fraction is very difficult to measure directly, it can be calculated from the overall volume fraction V_o and the calculated mesoscale volume fraction V_g . The overall volume fraction V_o was obtained from experimental data [9] for the three laminate configurations and it is reported in Table 3. Experimental values of V_o can be obtained from ignition loss method (ASTM D2854), acid digestion (ASTM 3171), or solvent extraction (ASTM C613). V_o is the product of the mesoscale volume fraction V_g and tow volume fraction V_f . The mesoscale volume fraction can be obtained from the solid model as the ratio of tow volume to RVE volume

$$V_g = \frac{v_y}{v_{rve}} \quad (3)$$

Therefore, the microscale (tow) volume fraction can be obtained as

$$V_f = \frac{V_o}{V_g} \quad (4)$$

both of which can be calculated by I-DEASTM or ANSYSTM from the respective solid models. Here, V_g is the mesoscale volume fraction obtained from the geometric model, V_f is the micro scale fiber volume fraction used for calculating the material properties of the composite tows, v_y is the total volume of the tows calculated from the geometric model, and v_{rve} is the volume of the RVE obtained from the geometric model. The tow fiber volume fraction V_f calculated from above equations did not match the V_f reported in [9]. The mesoscale volume fraction V_g from our solid model was too low because the rotation of the tows resulted in a slight increase in thickness of the RVE. This is accounted for by calculating the correct mesoscale volume fraction V'_g using the original dimensions of RVE, as follows

$$V'_g = \frac{v_y}{v'_{rve}} \quad (5)$$

and recalculating the tow fiber volume fraction

$$V'_f = \frac{V_o}{V'_g} \quad (6)$$

where V'_g is the corrected mesoscale volume fraction, v'_{rve} is the correct volume of RVE from measured data [9], and V'_f is the correct fiber volume fraction of the tow, as shown in Table 3.

Table 3
Overall, Mesoscale, and Microscale fiber volume fraction and laminate thickness for all configurations

	CERL	Scida [8] sinusoidal	Scida [8] elliptical	Single lamina [9]	Iso-phase laminate [9]	Out-of-phase laminate [9]
V_o (experimental)	0.3552	0.5500	0.5500	0.4400	0.4400	0.4400
V_g (FEM)	0.4909	0.6200	0.6510	0.5716	0.5716	0.5716
V'_f (Eq. (6))	0.71	0.5000	0.8000	0.6800	0.6800	0.6800
h' [mm] (experimental)	0.4251	0.1000	0.1000	0.6360	4.9900	4.8500
h [mm] (FEM)	0.4800	0.1040	0.1075	0.7300	5.8000	5.7600

When a fiber volume fraction correction is necessary to account for discrepancies between the FEM and the photomicrographs measurements, the elastic moduli are adjusted as follows:

$$E'_x = \frac{V'_f}{V_g} E_x \quad (7)$$

where h' , h , are the experimental and FEM model thickness, respectively (Table 3). The material properties of the tows are calculated using micromechanics [18,19] with V'_f as fiber volume fraction. The elastic properties of constituent materials (fiber and matrix) for the CERL fabric are obtained from [1] and for the remaining materials from [9]. The tows are transversely isotropic and thus require only five properties (E_1 , E_2 , G_{12} , ν_{12} , ν_{23}). Then, the properties are assigned to the tow and matrix elements in ANSYSTM. The next step is to apply the boundary conditions and analyze the results.

Since AS4 carbon fiber is transversely isotropic, the elastic properties are calculated using periodic microstructure micromechanics for transversely isotropic fibers [19]. As an alternative to [19] while taking into account transversely isotropic fibers with a simple model [17], the following procedure is proposed. First, calculate E_1 using the warp fiber modulus E_{f1} and ν_{12f} of the fiber, and the elastic properties of matrix. Next, cal-

culate E_2 using the radial fiber modulus E_{f2} and ν_{12f} of the fiber, and elastic properties of matrix. Then, calculate G_{12} using the value of G_{12f} , ν_{12f} of the fiber and elastic properties of matrix. Finally, calculate G_{23} using E_{f2} , ν_{23f} of the fiber and elastic properties of matrix, where ν_{23f} is calculated from the transversely isotropic conditions. These properties are checked for the restrictions on elastic constants [1]. The results are compared with [19] that assumes fibers to be transversely isotropic and with [18], that uses only longitudinal fiber properties E_{f1} and ν_{12f} . The results obtained from the approximate procedure show good correlation with the micromechanics model for transversely isotropic fibers (Table 4). The elastic properties of the constituent materials and the overall properties of the tow (composite) are reported in Table 5.

5. Boundary, periodicity, and compatibility conditions

A representative volume element (RVE) encompassing one full wavelength in the warp and fill directions (two pitches, or $2a$, which is twice the length shown in Figs. 1 and 5), exhibits geometric and material periodicity. Therefore, it can be used to analyze the composite by imposing periodicity conditions on its boundary

Table 4
Comparison of micromechanics model predictions [18,19]

Model type	E_1 (GPa)	E_2 (GPa)	ν_{12}	G_{12} (GPa)	G_{23} (GPa)
Isotropic fiber [18]	151.36	15.89	0.268	6.50	5.90
Approximate transversely isotropic fiber	151.36	8.731	0.271	3.906	3.339
Exact transversely isotropic fiber [19]	151.36	9.041	0.272	3.89	3.365

Table 5
Elastic properties of the fiber, matrix and tow and geometry of the RVE

	Scida [8]	CERL	Chou and Ito [9]
Fiber	E-glass	Carbon AS4-D	Carbon AS4-D
E_f longitud. [GPa]	73	221	221
E_f transv. [GPa]	73	16.6	16.6
ν_f	0.20	0.26	0.26
Matrix	Vinyl ester	Vinyl ester	Vinyl ester
E_m [GPa]	3.4	3.4	3.4
ν_m	0.35	0.35	0.3
Tow data/model	[17]	[16–18]	[9,17,18]
V_f (tow)	0.8	0.77	0.68
E_1 [GPa]	59.095	171.80	151.36
E_2 [GPa]	21.087	24.23	9.04
ν_{12}	0.224	0.324	0.27
G_{12} [GPa]	8.599	9.076	3.89
G_{23} [GPa]	7.630	8.051	3.36
RVE geometry			
a [mm]	1.5 3.0	0.918 1.836	1.6080 3.216
b [mm]	1.5 3.0	0.918 1.836	1.5275 3.055
h [mm]	0.5375 1.075 (514)	0.240 0.48	0.3600 0.730

1.075 (ellipse)

[20]. For example, computation of inplane shear moduli G_{xy} requires the following boundary conditions on a periodic RVE

$$\begin{aligned} u_1(a_1, y, z) - u_1(-a_1, y, z) &= 0 \\ u_2(a_1, y, z) - u_2(-a_1, y, z) - 2a_1 &= 0 \\ u_3(a_1, y, z) - u_3(-a_1, y, z) &= 0 \\ u_1(x, a_2, z) - u_1(x, -a_2, z) - 2a_2 &= 0 \\ u_2(x, a_2, z) - u_2(x, -a_2, z) &= 0 \\ u_3(x, a_2, z) - u_3(x, -a_2, z) &= 0 \\ u_i(x, y, a_3/2) - u_i(x, y, -a_3/2) &= 0 \end{aligned} \quad (8)$$

where $2a_1$, $2a_2$, a_3 , are the dimensions of the periodic RVE and u_i are the displacement components, both described using a coordinate system with origin at the center of the RVE. The constraints described by Eq. (8) can be applied using constraint equations in ANSYSTM. These constraints effectively impose both periodicity boundary conditions and an average strain γ_{xy}^0 equal to one to the RVE. However, periodicity conditions such as described by Eq. (8) are not easy to apply to FEM discretizations because nodes on opposite faces of the RVE cannot be found in pairs with two identical coordinates (y - z on warp faces and x - z on fill faces), but rather they are arbitrarily located as dictated by the free-mesh generation process.

A smaller RVE encompassing only one pitch (Figs. 1 and 5) in both the fill and warp directions can be carefully chosen to display symmetry conditions that can be easily imposed using standard FEA codes, as pro-

posed herein. This smaller RVE, of dimensions a_1 , a_2 , a_3 , encompasses only one-fourth the volume of the periodic one, thus yielding significant savings on computer time during the solution process.

For computation of the axial moduli and Poisson's ratios, symmetry conditions are imposed on one warp face (perpendicular to the warp tows) and on one fill face (perpendicular to the fill tows). Coupling conditions (CP) are used to keep the remaining warp and fill faces plane as they deform under load. This is necessary to avoid violating the symmetry conditions on those faces.

For computations of shear moduli, the displacements parallel to one warp face and one fill face are fixed while allowing unrestricted out-of-plane displacements on those faces. The displacements parallel to the surface on the remaining faces are coupled in order to apply an average shear strain γ_{xy}^0 on those faces while the out-of-plane displacements are unrestricted. Although the RVE encompasses only one-half period of the tow undulation, the resulting deformations are periodic as shown in Fig. 8. Although the shear stress and strain are not uniform inside the RVE, average values can be computed directly from the applied boundary conditions. Taking the computation of inplane shear modulus as an example, when displacements u_1 , u_2 are applied on two faces (Fig. 9), the average shear strain is

$$\gamma_{xy}^0 = u_1(x, a_2, z)/(a_2) + u_2(a_1, y, z)/(a_1) \quad (9)$$

and the resultants f_1, f_2 of the reaction forces on the other two faces yield the average shear stress

$$\sigma_{xy}^0 = \frac{f_1(y=0)}{a_1 a_3} = \frac{f_2(x=0)}{a_2 a_3} \quad (10)$$

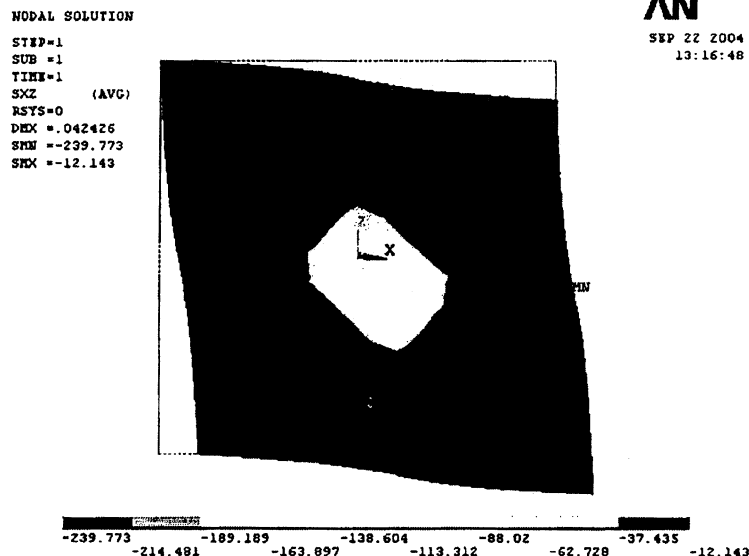


Fig. 8. Shear deformation and stress in the plane of the lamina under shear stress applied on the boundary.

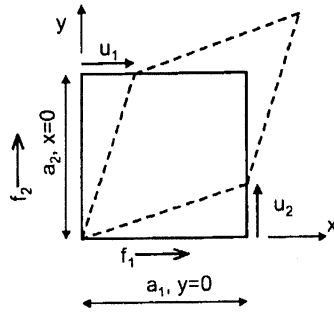


Fig. 9. Schematic of inplane shear deformation used to compute the inplane shear modulus from the numerical results of strain or stress on the boundary.

Elastic moduli can be computed by imposing either a uniform average stress (iso-stress) or uniform average strain (iso-strain). For computation of the axial moduli and Poisson's ratios, iso-stress conditions are applied by imposing a concentrated force to one face at a time, while displacements in the direction of the force are coupled so that the applied force effectively translates into an average stress. All remaining faces are let free but coupled so that their deformation remains plane. This results in a set of displacements that, by virtue of the coupling conditions, results in a set of average strains. For computation of shear moduli, pairs of congruent faces are loaded, one pair at a time, while the displacements parallel to each loaded face remain coupled. The computed values of average strain along with the values of imposed average stress are used in the compliance constitutive equations

$$\begin{aligned} \varepsilon_x &= S_{xx}\sigma_x & \varepsilon_y &= S_{yy}\sigma_y & \gamma_{xy} &= G_{xy}^{-1}\sigma_{xy} \\ \varepsilon_y &= S_{yx}\sigma_x & \varepsilon_z &= S_{zy}\sigma_y & \gamma_{xz} &= G_{xz}^{-1}\sigma_{xz} \\ \varepsilon_z &= S_{zx}\sigma_x & \varepsilon_x &= S_{zz}\sigma_z & \gamma_{yz} &= G_{yz}^{-1}\sigma_{yz} \end{aligned} \quad (11)$$

to compute the components of the stiffness tensor $[S]$ and from it all the moduli, as follows:

$$\begin{aligned} E_x &= 1/S_{xx} & \nu_{yz} &= -S_{zy}E_2 & G_{yz} &= 1/S_{yz} \\ E_y &= 1/S_{yy} & \nu_{xz} &= -S_{xz}E_1 & E_{xz} &= 1/S_{xz} \\ E_z &= 1/S_{zz} & \nu_{xy} &= -S_{xy}E_1 & E_{xy} &= 1/S_{xy} \end{aligned} \quad (12)$$

For computation of the axial moduli and Poisson's ratios using iso-strain conditions, a uniform out-of-plane displacement is imposed to one face of the RVE at a time while restricting the displacement at all other faces. For computation of shear moduli using iso-strain conditions, a uniform displacement is applied parallel to the plane of each pair of congruent faces. This results in a set of reaction forces on the restrained faces that are easily converted into average stress. The resulting values of average stress along with the values of imposed average strain are then used in the stiffness constitutive equation to obtain the components of the stiffness tensor, as follows:

$$\begin{aligned} \sigma_x &= C_{xx}\varepsilon_x & \sigma_y &= C_{yy}\varepsilon_y & \sigma_{xy} &= C_{xy}\gamma_{xy} = G_{xy}\gamma_{xy} \\ \sigma_y &= C_{yx}\varepsilon_x & \sigma_z &= C_{zy}\varepsilon_y & \sigma_{xz} &= C_{xz}\gamma_{xz} = G_{xz}\gamma_{xz} \\ \sigma_z &= C_{zx}\varepsilon_x & \sigma_x &= C_{zz}\varepsilon_z & \sigma_{yz} &= C_{yz}\gamma_{yz} = G_{yz}\gamma_{yz} \end{aligned} \quad (13)$$

Then, the compliance tensor is computed as the inverse of the stiffness tensor $[S] = [C]^{-1}$. Finally, Eq. (12) is used to compute the elastic moduli and Poisson's ratios.

Both iso-strain and iso-stress conditions yield virtually identical results when applied to the FE model because the geometry of the meso-structure (tows) is represented in great detail and fully utilized by the FE model in the solution. Model predictions are compared to experimental values and other results from the literature in Table 6.

6. Approximate method

Classical lamination theory (CLT) can be used to obtain a quick estimate of the inplane moduli. Modeling the plain weave fabric as a laminate and computing the equivalent laminate moduli results in approximate values for the inplane stiffness properties of the fabric. The following method is proposed. The fill is represented by a center layer of unidirectional composite oriented at 90° and the warp by two outer layers oriented at 0° . The properties of the equivalent unidirectional composite laminae are found using micromechanics [18,19]

Table 6
Comparison of predicted and experimental elastic moduli of fabric reinforced laminates

Properties	Ref. [8]	FE model	PMM [17]	CLT
E_1 (GPa)	24.8 ± 1.1^a	24.439	25.1	27.4
E_2 (GPa)	24.8 ± 1.1^a	24.534	25.1	27.4
E_3 (GPa)	8.5 ± 2.6	10.253	10.5	-
G_{12} (GPa)	6.5 ± 0.8^a	5.515	4.37	3.846
G_{13} (GPa)	4.2 ± 0.7	3.151	2.91	-
G_{23} (GPa)	4.2 ± 0.7	3.159	2.91	-
ν_{23}	0.28 ± 0.07	0.382	0.34	-
ν_{13}	0.28 ± 0.07	0.380	0.34	-
ν_{12}	$0.1 \pm .01^a$	0.126	0.123	0.120

^a Experimental value, all other values in the same column as predicted in [8].

Table 7
Comparison of laminate inplane modulus E_x [GPa]

Geometry type	Type of laminate	Experimental	FEM prediction	PMM	CLT
CERL	Single lamina	N/A	40.9	39.12	46.66
Scida sinusoidal tow [9]	Single lamina	24.8 ± 1.1	27.1	24.9	27.40
Scida elliptical tow [9]	Single lamina	24.8 ± 1.1	26.5	24.9	27.40
Ito and Chou [10]	Single lamina	43.5 26.7	46.9 —	43.1 —	55.58
	Iso-phase laminate	42.8	41.5	N/A 43.1	55.58
	Out-of-phase laminate	51.8	49.5	N/A	55.58
Random		44.5			

and the known overall fiber volume fraction of the composite V_o . Then, a $[0/90_2/0]_T$ laminate is constructed and analyzed to find the equivalent laminate moduli, as explained in Section 6.4 of [1]. The thicknesses of the laminae are controlled by the arbitrary parameter t . The computations are performed using the software CADEC [1] and reported in column 4 of Table 6.

The overall fiber volume fraction is seldom available in design, when candidate materials have not been fabricated in order to measure V_o . In this case, V_o can be estimated by using [1]

$$V_o = \frac{w}{\rho_f h} \quad (14)$$

where w , ρ_f , h , are the weight of the dry fabric in g/m^2 , the fiber density in g/m^3 , and the anticipated thickness of the composite lamina in meters. The latter can be estimated as the thickness of the dry fabric as long as the fabrication process provides for good consolidation, excess resin bleeding, and entrapped air bleeding.

Rather than estimating the final laminate thickness, one can use the fabric pitch to calculate a good approximation to it. The tow pitch a is easy to measure as the inverse of the number of tows N in 1 m length of fabric. For example, the pitch of the fill tow is $a_2 = 1/N_w$ (Fig. 1). A cross section of lamina spanning one pitch a_1 , with area equal to $(a_1 a_3)$ contains the cross-section of one fill tow (two half tows in Fig. 1). The total weight of the fabric per unit (inplane) area is denoted by w (g/m^2). In a balanced plain weave fabric, fill tows account for half of the total weight of the fabric. Therefore, the area of one fill tow is

$$A_{fi} = \frac{(w/2)/N_w}{\rho_f} = \frac{wa_2}{2\rho_f} \quad (15)$$

The area of an ellipse is

$$A_e = \frac{\pi ab}{4} \quad (16)$$

where a , b , are the major and minor axes of the ellipse. Assuming an elliptical cross-section for the tow ($A_{fi} = A_e$), and assuming no spacing between tows ($a_g = 0$ in Fig. 5), the tow thickness is

$$b = \frac{2w}{\pi\rho_f} \quad (17)$$

Finally, the thickness of the warp and fill tows are identical for a balanced plain weave fabric. Therefore, the laminate thickness is simply

$$h = a_3 \cong 2b = \frac{4w}{\pi\rho_f} \quad (18)$$

The CLT predictions and reported in column 7 of Table 6. As seen in Table 6, the FEM model and the periodic microstructure model (PMM, [21]) predict the inplane moduli very well. CLT over predicts the inplane moduli because it does not account for the undulation. In CLT, all the fiber material is assumed to be flat, thus yielding an artificially high value. The remarkable accuracy of the PMM and FEM models is due to their accurate representation of the geometry of the tows and the directionality of the fiber properties along the undulation of the tows. CLT underestimates the inplane shear modulus by 41% when compared to experimental data. This is because CLT is a rule of mixtures model where the geometry of the mesoscale (tows) is poorly represented and it is well known that the rule of mixtures underestimates matrix-dominated properties such as shear moduli. The present FE model provides the best estimate of inplane shear moduli when compared to experimental data. The transverse properties reported by Scida [8] are not experimental values but predictions made by using a refined CLT model. While comparisons with lamina data are presented in Table 6, laminate data is shown in Table 7 to provide further evidence that the FE and PMM models outperform CLT in the prediction of inplane moduli.

7. Conclusions

A novel procedure is developed for representing the geometry of the tows and matrix in variety of laminate configurations including single, iso-phase, and out-of-phase laminates. The geometric model is based on microphotograph measurements that are translated into a solid model and an FEM model using commercial software. The elastic moduli of the plain weave fabric-reinforced laminates are obtained using finite element analysis. The values predicted by the FEM models compare favorably with the experimental values. The model is simple; as it is based on microphotograph

measurements and the stiffness values of a unidirectional composite that can be obtained from standard tests.

Acknowledgement

Partial support for this project provided by the Construction Engineering Research Laboratory through contract DAC42-01-C-0033 is gratefully acknowledged.

References

- [1] Barbero EJ. Introduction to composite materials design. Philadelphia, PA: Taylor and Francis; 1999.
- [2] R. Pandey. Micromechanics-based computer-aided design and analysis of two-dimensional and three-dimensional fabric composites. Dissertation, Pennsylvania State University, PA; 1995.
- [3] Huang ZM. The mechanical properties of composites reinforced with woven and braided fabrics. *Compos Sci Technol* 1999;60: 479–98.
- [4] Naik NK, Ganesh VK. Prediction of on-axes elastic properties of plain weave fabric composites. *Compos Sci Technol* 1992;45: 135–52.
- [5] Vandeurzen Ph, Ivens J, Verpoest I. A three-dimensional micromechanics analysis of woven-fabric composites: I. Geometric analysis. *Compos Sci Technol* 1996;56:1303–15.
- [6] Vandeurzen Ph, Ivens J, Verpoest I. A three-dimensional micromechanics analysis of woven-fabric composites: II. Elastic analysis. *Compos Sci Technol* 1996;56:1317–27.
- [7] Hahn HT, Pandey R. A micromechanics model for thermo-elastic properties of plain weave fabric composites. *J Eng Mater Technol* 1994;116:517–23.
- [8] Scida D, Aboura Z, Benzeggagh ML, Bocherens E. A micromechanics model for 3D elasticity and failure of woven-fiber composite materials. *Compos Sci Technol* 1999;59:505–17.
- [9] Chou TW, Ito M. An analytical and experimental study of strength and failure behavior of plain weave composites. *J Compos Mater* 1998;32:2–30.
- [10] Ishikawa T, Chou TW. One-dimensional micromechanics analysis of woven fabric composites. *J Am Instit Aeronaut Astronaut* 1983;21:1714–21.
- [11] Ishikawa T, Chou TW. Stiffness and strength behavior of woven fabric composites. *J Mater Sci* 1982;17:3211–20.
- [12] Aitharaju VR, Averill RC. Three-dimensional properties of woven-fabric composites. *Compos Sci Technol* 1999;59:1901–11.
- [13] Blackletter DM, Walrath DE, Hansen AC. Modeling continuum damage in a plain weave fabric-reinforced composite material. *J Compos Technol Res* 1993;15:136–42.
- [14] Kollegal MG, Sridharan S. Strength prediction of plain woven fabrics. *J Compos Mater* 1998;34:241–57.
- [15] Kollegal MG, Sridharan S. A simplified model for plain woven fabrics. *J Compos Mater* 1998;34:1757–85.
- [16] Trovillion J. Construction Engineering Research Lab, CERL, Urbana-Champaign, Illinois, Private Communication; 2002.
- [17] Barbero EJ, Damiani TM, Trovillion J. Micromechanics of fabric reinforced composites with periodic microstructure. *Int J Solid Struct* 2005;42:2489–504.
- [18] Barbero EJ, Luciano R. Formulas for the stiffness of composites with periodic microstructure. *Int J Solid Struct* 1994;31: 2933–43.
- [19] Barbero EJ, Luciano R. Micromechanics formulas for the relaxation tensor of linear viscoelastic composites with transversely isotropic fibers. *Int J Solid Struct* 1995;32:1859–72.
- [20] Luciano R, Sacco E. Variational methods for the homogenization of periodic heterogeneous media. *Eur J Mech Solids* 1998;17(4): 599–617.
- [21] Damiani T. Ph.D. Dissertation, West Virginia University; 2003.